PLOS COMPUTATIONAL BIOLOGY

RESEARCH ARTICLE

Tuning collective behaviour in zebrafish with genetic modification

Yushi Yang[1,2], Abdelwahab Kawafi[3], Qiao Tong[3], Erika Kague[3,4], Chrissy L. Hammond[3], C. Patrick Royall[5]*

1 H. H. Wills Physics Laboratory, University of Bristol, Bristol, United Kingdom, **2** Bristol Centre for Functional Nanomaterials, University of Bristol, Bristol, United Kingdom, **3** Department of Physiology, Pharmacology, and Neuroscience, Medical Sciences, University of Bristol, Bristol, United Kingdom, **4** Institute of Genetics and Cancer, Centre for Genomic and Experimental Medicine, University of Edinburgh, Crewe Road South, Edinburgh, United Kingdom, **5** Gulliver UMR CNRS 7083, ESPCI Paris, Université PSL, Paris, France

* paddy.royall@bristol.ac.uk

Check for updates

OPEN ACCESS

Citation: Yang Y, Kawafi A, Tong Q, Kague E, Hammond CL, Royall CP (2024) Tuning collective behaviour in zebrafish with genetic modification. PLoS Comput Biol 20(10): e1012034. https://doi.org/10.1371/journal.pcbi.1012034

Editor: Christopher Rao, University of Illinois at Urbana-Champaign, UNITED STATES OF AMERICA

Received: April 16, 2024

Accepted: September 24, 2024

Published: October 28, 2024

Copyright: © 2024 Yang et al. This is an open access article distributed under the terms of the Creative Commons Attribution License, which permits unrestricted use, distribution, and reproduction in any medium, provided the original author and source are credited.

Data Availability Statement: Representative data is available here: https://zenodo.org/records/10693744. Simulation code is available on GitHub (https://github.com/yangyushi/FishSim).

Funding: YY was funded by the China Scholarship Council for funding. EK was funded by Versus Arthritis (Career Development Award, 23115). CPR was funded by European Research Council (ERC consolidator grant NANOPRS, project 617266). CPR acknowledges the Agence Nationale de Recherche for the grant DiViNew. The funders had no role in study design, data collection and

Abstract

Zebrafish collective behaviour is widely used to assess their physical and mental state, serving as a valuable tool to assess the impact of ageing, disease genetics, and the effect of drugs. The essence of these macroscopic phenomena can be represented by active matter models, where the individuals are abstracted as interactive self-propelling agents. The behaviour of these agents depends on a set of parameters in a manner reminiscent of those between the constituents of physical systems. In a few cases, the system may be controlled at the level of the individual constituents such as the interactions between colloidal particles, or the enzymatic behaviour of *de novo* proteins. Usually, however, while the collective behaviour may be influenced by environmental factors, it typically cannot be changed at will. Here, we challenge this scenario in a biological context by genetically modifying zebrafish. We thus demonstrate the potential of genetic modification in the context of controlling the collective behaviour of biological active matter systems at the level of the constituents, rather than externally. In particular, we probe the effect of the lack of *col11a2* gene in zebrafish, which causes the early onset of osteoarthritis. The resulting *col11a2 -/-* zebrafish exhibited compromised vertebral column properties, bent their body less while swimming, and took longer to change their orientations. Surprisingly, a group of 25 mutant fish exhibited more orderly collective motion than the wildtype. We show that the collective behaviour of wildtype and *col11a2 -/-* zebrafish are captured with a simple active matter model, in which the mutant fish are modelled by self–propelling agents with a higher orientational noise on average. In this way, we demonstrate the possibility of tuning a biological system, changing the state space it occupies when interpreted with a simple active matter model.

Author summary

Collective behaviour emerges across a very wide range of systems which span lengthscales of many orders of magnitude. Examples include phase transitions in atomic and molecular materials, and colloidal dispersions, and self-propelled particles. Recently universal

analysis, decision to publish, or preparation of the manuscript.

Competing interests: The authors have declared that no competing interests exist.

behaviour has been found connecting these physical systems to motile cells and groups of animals, such as the murmuration in Starlings.

The swimming of a group of Zebrafish can be described with surprising accuracy by self-propelled particles which follow very simple mathematical rules. This model exhibits an ordering transition in which all individuals travel in the same direction. Here we study the effect of genetic modification of their spines on the swimming of the Zebrafish. We find that the genetically modified fish take a longer time to make turns, and have a continuous range of swim speeds, while wild type fish turn tightly and tend to swim either slowly or quickly. Surprisingly, the mutant fish are also described by the very same model of self-propelled particles but under a slight change of parameter. This work shows that genetic modification can tune the dynamical behaviour of a biological system and this can be captured accurately with a very simple physical model.

Introduction

Animal groups exhibit a rich variety of collective behaviour, exhibiting complex patterns across different length scales, from a swarm of insects (centimeters) to large fish shoals (kilometers) [1–6]. Such collective motion may be interpreted as an emergent phenomena originating from interactions between individuals [7–9], which can be beneficial for the entire group [10–14]. Therefore, a reductionist way to approach such collective behavior is to treat the individuals as interacting self-propelling agents [15, 16]. In this sense, the animal group can be described as an *active matter* system [17–19]. Particular examples include flocking and schooling behavior of biological systems which can be reproduced in computer simulations [20–22], experiments with active colloids [16, 23, 24], as well as robotic swarms [25, 26]. Within the framework of a system comprised of many agents, or particles in the case of physical systems, the macroscopic behavior of the system can be controlled externally. In physical systems, state variables such as temperature drive phase transitions, or noise in agent trajectories leads to a dynamical ordering transition in active systems [15, 27, 28]. In biological systems collective behavior in schools of fish, for example, can be strongly influenced by predation [29] and swarms of midges may be controlled ambient lighting [6, 30].

What these diverse examples have in common is a system of individuals with certain characteristics which respond to an external change in the environment. However, another *bottom-up* approach is to tune the properties of each constituent. While often this is forbidden by nature (the immutable laws of quantum mechanics in the case of atoms) or impractical (it is hard to control large bird flocks for example [9]), some systems are amenable to the design of their constituents. For example, synthetic active colloids [16] are an idealised playground to understand the principles of active matter, exhibiting dynamical [24, 31, 32] or structural [33–35] transitions, complex plasmas constitute particulate systems with tunable behaviour [36], while the emergence of *de novo* proteins enables design of enzymatic behaviour [37].

Here we explore the possibility of tuning the collective behaviour in a biological system by changing the characteristics of the constituents in the bottom–up manner of the colloids and *de novo* proteins. For this purpose, we use the zebrafish system, which has a well-established collective behaviour that can be monitored in the laboratory by tracking the individual fish [38–40] and which is amenable to genetic modification [41–44]. Genetic modification has been shown to change behavioural patterns in groups of fish [45, 46]. By studying groups of mutant zebrafish, we can investigate how changes in individuals lead to collective behaviour and explore the underlying biological mechanisms that drive these emergent phenomena. The

collective behaviour of zebrafish can further be compared to well established active matter models that encapsulate single fish properties [47–49], fish–fish interactions, [15, 20] as well as the interaction between fish and the environment [50, 51].

In particular, we investigated the behaviour of zebrafish carrying a *homozygous* deleterious mutation in the *col11a2* gene (*col11a2*-/-), that is to say, both parents exhibited the same mutation. These mutant fish exhibited abnormal skeletal development [52]. We also observed several degenerative defects in their vertebral column, including vertebral fusions and ruptures of the intervertebral discs. Therefore, we expect the mutation in *col11a2* to change the zebrafish swimming dynamics compared to the wildtype. Interestingly, we found that the *col11a2* mutant zebrafish exhibited limited vertebral column bending during swimming, and they took a significantly longer time to change their swim direction than wildtype. Surprisingly, a group of 25 mutant zebrafish exhibited a more polarised swimming pattern. These behavioral differences are well explained by the Vicsek model with a simple modification on the orientation updating rule [15, 40], suggesting that the *col11a2* mutant zebrafish exhibits reduced behavioral noise. Such reduction can be attributed to the limited bending of their bodies, intrinsically related to their vertebral defects. In this way, when interpreted through a simple active matter model, the state space accessed by the fish is controlled at the level of each individual in a manner analogous to simple tunable systems such as colloids.

Materials and methods

Ethics statement

The wild–type zebrafish and the mutant fish were bred and kept in the fish facility in the university of Bristol, following standard procedures [53]. Our behaviour experiments were approved by the local ethics committee (University of Bristol Animal Welfare and Ethical Review Body, AWERB) with a UIN (university ethical approval identifier). *col11a2* sa18324 mutant zebrafish have a C > A base pair change at position 228, which leads to a premature stop codon the triple helical domain of the $\alpha 2$ chain of collagen 11.

Micro-computed tomography (μCT) and bone density analysis

Adult zebrafish (6 and 12-month-old) were fixed in 4% PFA for one week and sequentially dehydrated to 70% ethanol. After fixation, full body scans were taken with a voxel size of 20 μm, using a Nikon XT H 225ST μCT scanner (x-ray source of 130 kV and 53 μA without additional filters). The generated scans were then reconstructed using Nikon CT Pro 3d software. During reconstruction, greyscale values were calibrated against a scan of a phantom with known density (0.75 gcm^{-3}) using the exact same settings. Calibrations with the phantom were used to calculate bone density. Morphological analyses were performed using Avizo software (FEI) and volume rendering function. Tissue Mineral Density (TMD) was calculated based on the segmentation of the centra from caudal vertebrae (position 1-3).

Alizarin Red staining

Alizarin Red staining was performed on 1-year-old zebrafish, as previously described [54]. Pictures were taken using a Leica Stereomicroscope (DM4000) with a 580 excitation filter.

Sections for Toluidine Blue imaging

Adult fish (1-year-old) were fixed in 4% paraformaldehyde (PFA) for 14 days, then decalcified in 1M Ethylenediaminetetraacetic acid (EDTA) solution for 20 days at room temperature. Samples were dehydrated to ethanol, embedded in paraffin, and sagittal sections at 8 μm

thickness were taken. Selected slides were de-waxed and stained with Toluidine Blue [55]. Images were acquired on a Leica DMI600 inverted microscope, using 20X and 40X oil objectives, LAS software, and a DFC420C colour camera.

Second Harmonic Generation (SHG)

Dissected spines of wild–type and *col11a2* -/- zebrafish (1-year-old) were mounted in 1% low-melting point agarose (n = 3 for each group) and SHG imaged acquired using 25x/0.95 water dipping lens, 880nm laser excitation, and simultaneous forward and backward detection (440/20) with a Leica SP8 AOBS confocal laser scanning microscope attached to a Leica DM6000 upright epifluorescence microscope with multiphoton lasers allowing fluorescent and SHG acquisition of the same sample and z-stack. Microscope parameters for SHG acquisition were set as previously described [56].

2d tracking apparatus

We used one camera (Basler ac2040um) to capture the motion of a single fish at a rate of 15 frames per second. The camera was mounted on top of the fish tank, which offered a shallow (5 cm) water environment for the fish. Since it is challenging to mount camera perfectly perpendicular with respect to the water surface, we further rectified the obtained image following the method introduced in [57] by capturing an image with a chessboard floating on top of the water surface. We segmented the pixels corresponding to the single fish and took the centre as the 2d fish location. The locations in different time points were connected to form the trajectories.

3d tracking apparatus

We used three synchronised cameras (Balser ac2040 um) to capture the motion of the fish at a rate of 15 frames per second. The intrinsic parameter of the cameras was calibrated with a standard chessboard pattern. The extrinsic parameters, containing the location and orientation of the cameras, were calculated from a chessboard pattern floating on the water surface. The results were then optimised by enforcing a geometric constraint from the tank, whose shape is known.

The observation setup is composed of a white bowl-shaped container (referred to as the observation tank), which was immersed in a circular paddling pool. The water temperature of the observation tank was maintained around 25˚C by heaters in the paddling pool, and we placed two filters in the paddling pool to control the water quality.

The fish were transferred from their living tank to the observation tank before each experiment. The video recording started 5 minutes after the transfer, and the room was evacuated for 5 minutes. The water in the observation tank was still during the observation, and we circulated the water when the fish were not being observed.

Data processing

We explicitly considered the projective geometry to calculate the 3d locations of the fish from their corresponding images from different cameras [57]. During the calculation, we considered the refraction of light at the water-air interface, following our previous method [40]. We linked the 3d locations into short trajectories following a four-frame method [58], and extended these trajectories following the idea of Xu [59]. We take the time difference of locations as velocities and the directions of the velocities as the fish orientations. The autocorrelation function of the orientations was calculated to determine the reorientation time. The code for our image

process and correlation analysis is available as an open-source project on GitHub (https://github.com/yangyushi/FishPy).

For the swimming posture analysis, we segmented the fish from the background in the image captured by the camera. The segmentation was performed by setting all pixels whose intensity values are below the threshold value to background pixels. We aligned the orientation of the fish by rotating the principal axes of the foreground pixels, so that these axes align with the X and Y axis of the image. The segmented and aligned image contain one fish, with the size of 50×50 pixels. We then concatenated all the 37,985 aligned images, from both the wild–type fish and the mutant fish across different observations in a quasi-2d environment, into a single array with a shape of $37,985 \times 50 \times 50$. The array was then flattened into shape $37,985 \times 2500$ for the PCA. Effectively, we analysed a dataset with 2500 features and 37, 985 samples.

Simulation details

We simulated a variation of the Vicsek model proposed in [40] whose equation of motion is given by Eq 2. To fit the experimental data to this inertial Vicsek Model, we changed the value of the noise parameter η from 0.5 to 1.0, while fixing the values of other variable ($v_0 = 0.1$, $\rho = 0.5$, $\alpha = 0.63$). These fixed parameters also fits the behaviour of 50 adult zebrafish, except for the value of the density (we set $\rho = 1$ for 50 adult fish). The consistent fit suggests our proposed model, regardless its simplicity, does capture the essence of the collective behaviour of zebrafish.

We use our custom Python library to carry out the simulation of the inertial Vicsek model. To fit our experimental results, we set the inertial term (α) to be 0.63, the number density (ρ) to be 0.5, and the speed (v_0) to be 0.1. The agents were confined by a cubic box with periodic boundary conditions. We carried out simulations at different noise intensity values ranging from 0.65 (less noisy) to 1.0 (completely random). At each noise value, we prepared the system with random locations and random orientations. We waited for 10^5 simulation steps for the system to reach a steady state and sampled another 10^5 steps to collect data for statistical analysis. The simulation library is available as an open-source project on GitHub (https://github.com/yangyushi/FishSim).

Results

We bred genetically modified zebrafish whose *col11a2* gene is *knocked out*, such that the functional product of this gene is lacking, and compared the biological features of mutants to wild-type siblings. We found that the vertebral column of mutant fish displayed abnormal vertebrae. Additionally, they showed irregular shape of otoliths (mineralised rods located in the fish ears, which help them sense position), see section I in S1 Text. Because these abnormalities could modify the dynamics of *col11a2* -/- fish, we expect that the collective behaviour of the system may be modified at the level of single fish. To probe our hypothesis, we investigate the fish in two environments. Firstly, in a quasi–2d situation in which the fish are confined within a height of 5 cm, with a particular focus on their postures. We found that the *col11a2* -/- zebrafish showed significantly reduced bending compared to the wildtype. Then, in a 3d swimming environment, we recovered the 3d trajectories of fish swimming alone ($N = 1$) or swimming as a group ($N = 25$) with a custom three view tracking apparatus [40, 57, 60]. Strikingly, a single mutant fish took a significantly longer time to change its orientation, and a group of *col11a2* -/- zebrafish exhibited more ordered movement characterised by the polarization order parameter. The differences between wild–type and col11a2 mutant fish are summarised in Table 1. By comparing our experimental data with numerical simulation of a modified Vicsek model, we found that the behavioral difference between mutant fish and wild–type fish

Table 1. A summary of the difference between the wild–type and the col11a2-/- zebrafish.

Difference	Distinct features of the col11a2-/- zebrafish	Source
Intervertebral discs	Disorganised and ruptured structures	Fig 1
Otoliths	Irregular shapes and lower density	Fig S1 in S1 Text
Swimming posture	Less bending while swimming	Fig 2
Swimming dynamic	Takes longer time to change the swimming direction	Fig 3F and 3H
Swimming Speed	A different speed distribution	Fig 3E and 3G
Swimming Location	Prefer swimming near the water–air interface	Fig 3C and 3D
Collective Behaviour	More ordered movement in a group of twenty five	Fig 3I

https://doi.org/10.1371/journal.pcbi.1012034.t001

is well captured by the model where on average *col11a2 -/-* zebrafish have lower orientational noise.

The *col11a2 -/-* zebrafish exhibit defects in their vertebral column

To characterise the biological difference between the *col11a2 -/-* zebrafish and their corresponding wild–type controls, we performed skeletal phenotyping to identify changes associated with bone and cartilage in the vertebral column. First, we performed micro-computed tomography of adult (6-month-old) zebrafish which provides a 3d reconstruction of the fish skeleton. Strikingly, *col11a2 -/-* zebrafish ($n = 16$) commonly showed multiple vertebrae fusions associated with the caudal region of the axial skeleton. Such fusions compromised from 2 to up to 5 adjacent vertebrae, as shown in Fig 1A. Using Alizarin Red staining, which labels calcified tissues and allows a detailed visualisation of the small zebrafish bones, we further detected bone abnormalities associated with the vertebral bodies and vertebral arches, exhibited in Fig 1B.

Intervertebral discs that separate one vertebrae from each other are the most important vertebral element to allow spine flexibility and serve as shock-absorbing cushions under mechanical load and vertebral column movement [61]. In mammals and fish, the intervertebral disc is formed by the nucleus pulposus internally (formed by fibrous tissue and cartilage-like cells) and externally at the bone junction by the annulus fibrosus composed of collagen and elastin layers [44] (Fig 1c). To assess the structure of the intervertebral discs at the cellular level, we imaged sections of the wild–type and mutant fish, which were stained with by Toluidine Blue (which labels soft tissue), as shown in Fig 1C. Here, tissue slices of 8μm in thickness throughout the vertebral column were imaged. The regions forming the intervertebral discs are shown in the schematics. At lower magnification, the annulus fibrosus and nucleus pulposus can be observed (left panel). The nucleus pulposus is formed by cartilage-like cells and fluid. While the annulus fibrosus is formed by layers of elastin and collagen fibers. At higher magnification with a focus on the annulus fibrosus (right panel), the layers of collagen and elastin that form the annulus fibrosus can be observed in detail. These regions are well defined in the wild type fish but are very disorganized in the mutants. Strikingly, the higher resolution images (Fig 1C, right) show a region of elastin that is ruptured in the mutant sample (indicated with an arrow). In other words, the most dramatic changes found in *col11a2 -/-* fish were associated with the annulus fibrosus (Fig 1C). The collagen layers that compose the annulus fibrosus are abnormal, and the elastin layer, which allows flexibility to the intervertebral disc and the vertebral column, is ruptured. The nucleus pulposus is more fibrous than normal; however, these differences are not dramatic. Our results demonstrate that the lack of *col11a2* leads to a destabilization of the intervertebral discs and the elasticity of the vertebral column.

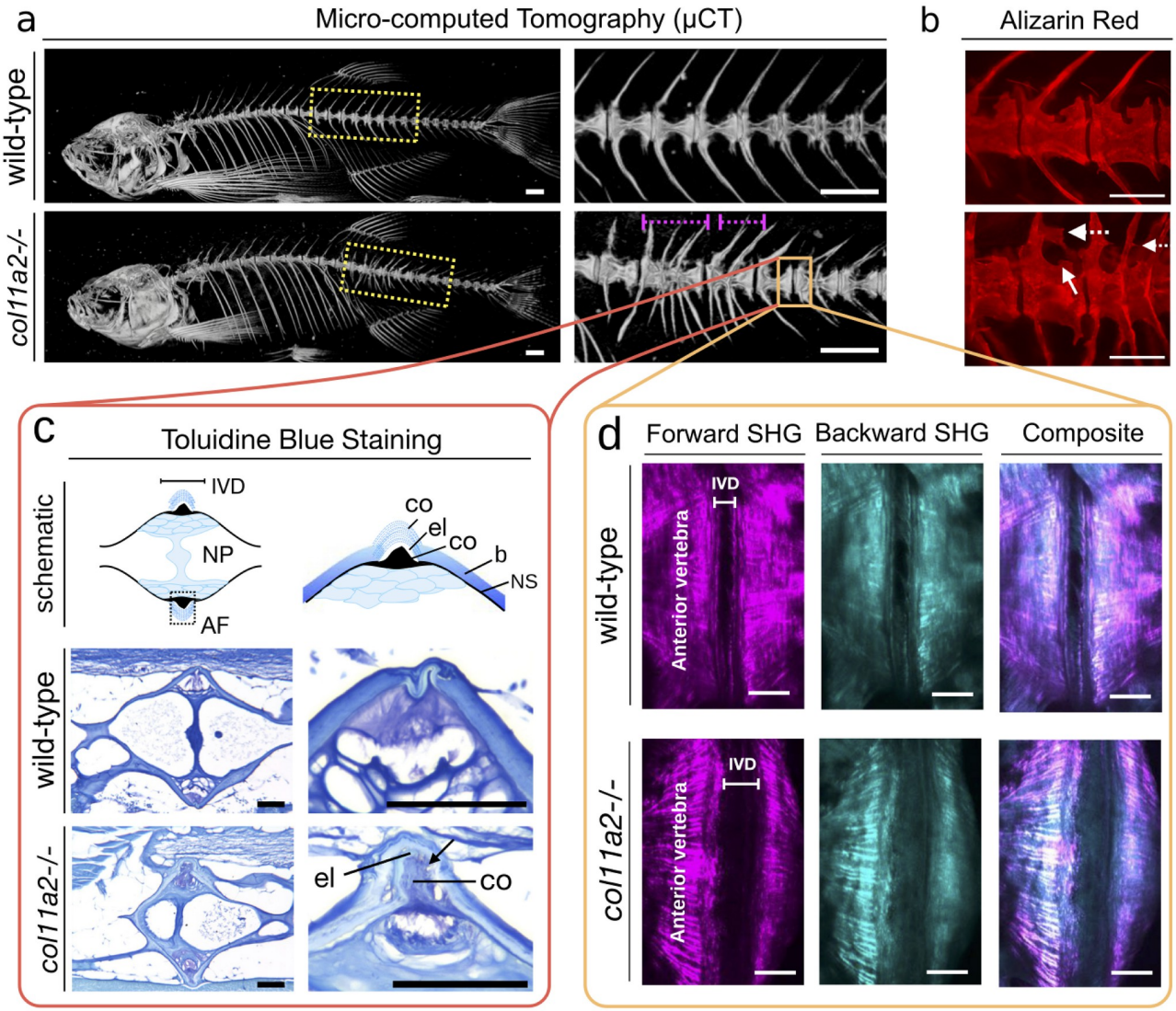

Fig 1. Effects of *col11a2*-/- knockout in zebrafish. The *col11a2* -/- zebrafish have a fused vertebral column, ruptured annulus fibrosus and morphological abnormalities. (a) Micro-computed Tomography (μCT) of 6-month wild–type and mutant fish. The region highlighted with dashed yellow box is shown with higher magnification on the right panel. Note vertebrae fusions (magenta dash lines). (b) Fluorescent microscopic images of the calcified tissues of zebrafish labelled by Alizarin Red staining. Note abnormal vertebral trabeculations (arrow) and bone outgrowths from the arches (dashed arrow). Scale bars = 500 μm. (c) Toluidine blue stained images showing the cellular components of the soft tissue intervertebral disc (IVD) region. The top schematic (left) shows the encounter of two vertebrae at the IVD region, with the annulus fibrosus (AF) and nucleus pulposus (NP) annotated. The top right schematic shows a higher magnification view of the annulus fibrosus (AF) region, which is formed by an external layer of collagen fibres (co), an elastin layer (el) and another collagen rich region (co). The vertebral bone (b) and the notochord sheath (ns) are annotated. The sections of the wild–type and *col11a2* -/- fish are shown in the middle and bottom rows respectively. Note that the elastin (el) and the collagen (co) layers are ruptured (arrow). (d) Forward and backwards Second Harmonic Generation (SHG) images of the wild–type and *col11a2* -/- zebrafish intervertebral disc area. Note thicker collagen fibres at the endplates (dashed line) of mutant fish. Disorganised collagen fibres in the IVD (AF) is detected in mutants (arrowhead) Scale bars = 50μm.

https://doi.org/10.1371/journal.pcbi.1012034.g001

To better visualize collagen fibers associated with the annulus fibrosus, we imaged the fish vertebral column using second harmonic generation microscopy, a non-linear infra-red microscopy technique. Such microscopy is sensitive to molecular alignment, and therefore provides a method to examine the 3d architecture of the fibrillary collagen matrix [44, 56, 62]. Forward (transmission) mode and backward (backscattered) second harmonic generation

microscopy are shown in Fig 1D, which reveal significant changes in collagen organization at the verebral endplates (edges of the bones at the vertebra) of mutants. Specifically, we detected uneven endplates associated with increased thicker fibers of collagen at the annulus fibrosus interface. While in the annulus fibrosus region, disorganized thin collagen fibers were detected (Fig 1D). Such dramatic changes in the organization of collagen fibers likely add to the flexibility impairment of the vertebral column during bending.

Our morphological assessment of the wild–type and *col11a2 -/-* zebrafish from 3d micro-computed tomography images revealed another biological difference, an irregular morphology for the otoliths (small calcified rod-like structures inside the inner ear of the fish), presented in section I of S1 Text. Otoliths are important in the regulation of balance during swim. Together, these observations characterise the structural difference of skeletons between mutant fish and wild–type, strongly supporting the biological foundation for the observed behavioral differences.

Quasi 2d swimming: Mutants have limited vertebral column bending

To understand the impact that the vertebral column had on swimming behavior, we analysed their swimming posture by placing individual zebrafish in the quasi 2d environment and used a camera above to capture videos while they swim, as illustrated in Fig 2A and 2B. In these videos, the fish appear as an elongated ellipse that bends every now and then, as illustrated in the sequence of images in Fig 2C. From our videos, we represent the shape of the fish with an image of w by w pixels, and flatten it into a w^2 dimensional vector for each of the m images. In this way, we obtain a dataset of shape $\mathbf{X} \in \mathbb{R}^{m \times w^2}$, and performed principal component analysis (PCA) to extract the characteristic modes of the fish shape. Specifically, we calculated the covariance matrix $\mathbf{C} = \mathbf{X}^\top \mathbf{X}$, and then calculated all the eigenvectors of $\mathbf{C}$. Typically, the eigenvector corresponding to the second largest eigenvalue of the covariance matrix describes the

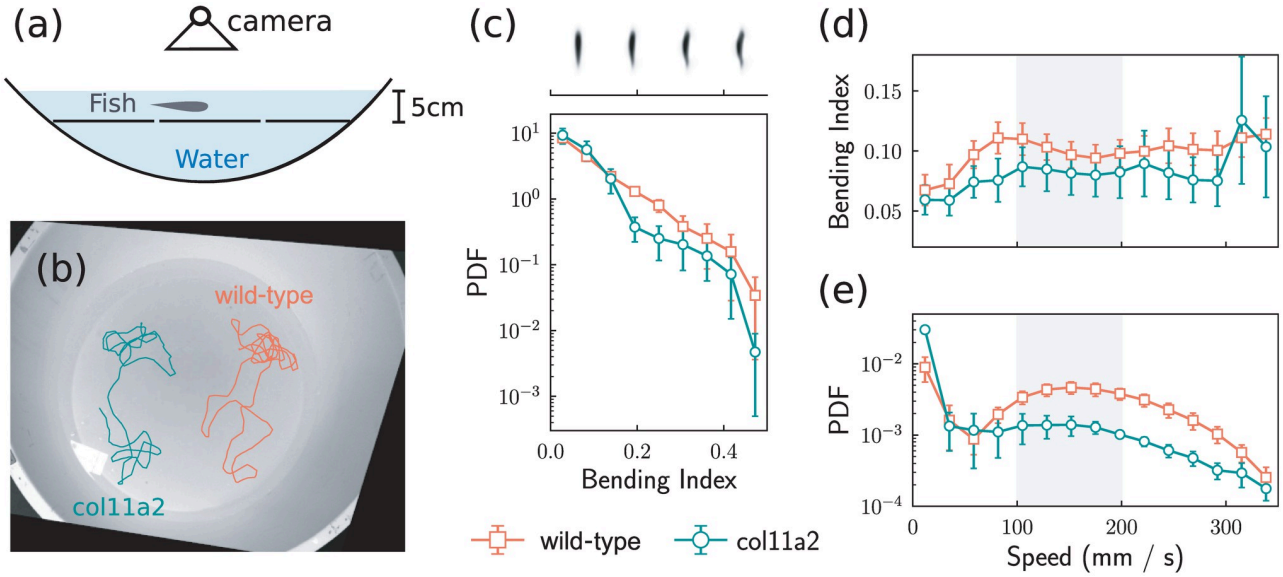

Fig 2. Differential swimming shape analysis of *col11a2 -/-* zebrafish. (a) illustration of our experimental setup for recording the 2d movement of fish. (b) Typical trajectories of mutant fish and wild–type fish replotted on top of the captured image. (c) Distribution of the bending index calculated from the image of the fish. The top panel, sharing the same x-axis with respect to the distribution plot, shows the characteristic shapes at different bending index values. (d) Average bending indices, calculated from the images of the fish shapes, for the wild–type fish and the mutant fish at different speed values. (e) Distribution of the speed values. Error bars represent the standard error calculated from 5 different fish.

https://doi.org/10.1371/journal.pcbi.1012034.g002

bending of the fish, and we term this eigenvector the *bending mode* **b**. We can, therefore, gauge the level of bending by projecting the fish shape ($\mathbf{x} \in \mathbb{R}^{w^2}$) onto the bending mode **b** by simply taking the dot product, $\mathbf{x} \cdot \mathbf{b}$. This quantity is termed the *bending index*. A more detailed description of the PCA analysis and the visualisation of different modes are available in section II of S1 Text.

The resulting posture analysis is shown in Fig 2C–2E where we focus on the bending index of the mutant fish and the wild–type fish. The mutant fish exhibit less bending compared to the wild–type fish, as shown in Fig 2C, indicated by the broader distribution of the bending index for the wild–type fish, as a result of "burst-and-coast" swimming style typical of zebrafish [63]. Recalling the discussion of Fig 1 above, it is also likely that the mutant joints are "stiffer" than those of the wild–type, due to the defective elastin layer of intervertebral discs, so they favor swimming in a way that involves less bending.

The relationship between the bending index and the swimming of the fish is also informative, as plotted in Fig 2D and 2E. The bending index of the wild–type fish reaches a maximum when they swim at speed around 100 mms^{-1}, exhibiting decreased bending as their speed further increased from 100 mms^{-1} to 200 mms^{-1}. This result explains the speed distribution of the wild–type fish, typically the bimodal shape that revealed a preferred swimming speed at around 150 mms^{-1}, shown in Fig 2E. Such a speed is preferred, possibly because in this speed range, they bend less and therefore use less energy. For the mutant fish, the correlation between the bending index and the swimming speed is rather different. The mutant fish exhibit smaller bending indices in speed regions from 0 to 300 mms^{-1}, and their bending index varies less with respect to the speed, compared to the wild–type. The observed bending index of mutant fish also explained their speed distribution, particularly the lack of a bimodal shape. Specifically, the mutant fish do not have the swimming posture, that allows them to enjoy a higher speed while performing less bending, therefore, they do not have a preferred swimming speed. Importantly, we did not observe any behaviour changes that suggested an altered balance of the fish during the swim. Collectively, regardless of the various possible effects on the collective behavior associated with the mutants, we concluded that the vertebral column abnormality is the major contributor to behavior changes leading to reduced flexibility in mutant fish, which resulted in limited bending while swimming.

3d swimming: Mutants take longer to change their swimming direction

This characteristic difference in speed distribution for the mutant fish and the corresponding wild–type, can also be observed when the fish swim in a 3d environment. We used a three–view apparatus to record zebrafish movement in 3d, and calculated individual 3d trajectories, as previously described [40]. An illustrative sketch of the apparatus is shown in Fig 3A, with representative trajectories of mutant fish and the wild–type fish shown in Fig 3B. Specifically, we calculated 10 single–fish trajectories for both mutant fish and wild–type fish. We repeated the experiments with two different batches of fish, so that the batches are bred independently. Details of the experiments are available in section V of S1 Text.

The spatial distribution of individual wild–type and mutant fish is shown in Fig 3C. Individual fish tend to move near the wall of the tank, as seen in Fig 3C while few fish are distributed far from the tank wall. While the wild–type fish preferentially swim in the bottom region of the tank, the mutant fish are more likely to appear near the surface of the water. The wild–type exhibited their characteristic bimodal speed distribution in 3d, as shown in Fig 3E, while the mutant fish exhibited a single peak around 100 mms^{-1} in their speed distribution. Such a difference is consistent with the 2d experimental results (Fig 2C), suggesting the mutant fish

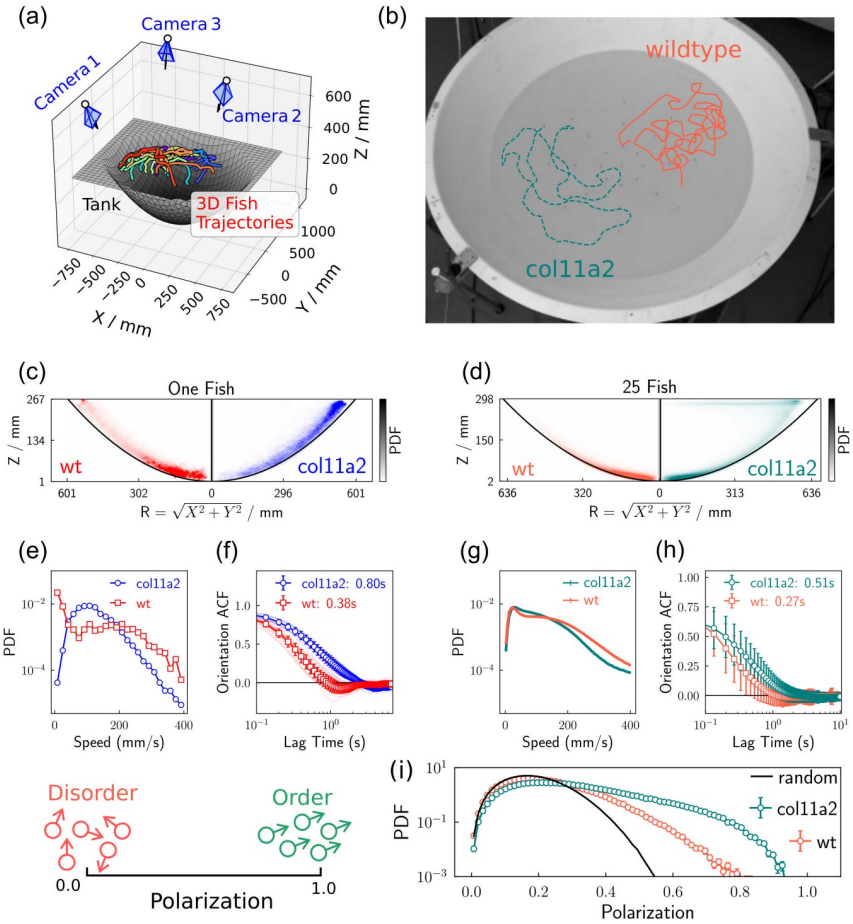

Fig 3. The behaviour of wild–type fish and mutant fish swimming in a three dimensional space. (a) A schematic of the experimental apparatus. The fish were placed in a bowl-shaped tank, and their movements were recorded by three synchronized cameras. The 3d trajectories of the fish were calculated from the recorded videos. The coloured line plots represent the movement of 25 mutant fish in 5 seconds. (b) The swimming trajectories for a single wild–type and a single mutant fish re–projected onto the recorded image, highlighting the difference in the persistence of the motion. (c, d) The joint probability distribution of the latitude radius (R) and the height (Z) of the wild–type fish and the mutant fish. (e, g) The probability distribution of the average swimming speed. (f, h) The averaged auto-correlation function of the fish orientation. (i) The probability distribution of the polarization order parameter (Eq 1), whose definition is illustrated on the left. The solid black line represents the polarization distribution of 25 randomly orientated vectors.

https://doi.org/10.1371/journal.pcbi.1012034.g003

also bend differently while swimming in 3d. (The direct measurement of body bending in 3d is beyond our current capacity, but it is in principle possible [64].)

We now characterise the dynamics of the fish in a quantitative manner, using the orientational autcorrelation function (ACF). Here we detect significant differences in the dynamics of orientation between mutant fish and the wild–type fish. The mutant fish took longer to change their direction, indicated by the auto–correlation function (ACF) of the moving direction of the fish, as shown in Fig 3E. The ACF depicts the temporal correlation of a random process at different time intervals, and we can use it to calculate relaxation time scales for both experiments and simulations [65].

Our analysis of zebrafish reorientation can be affected by several factors. For instance, the directional change of the non-moving individuals will be dominated by the tracking error. In

addition, an individual in the bottom of the tank will be forced to change direction more frequently, because the otherwise ballistic motion will be interrupted by the tank. To exclude these extrinsic effects, we excluded the non-moving time points in the trajectories (speed < 50 mms^{-1}), and focused only on a specific height region (50 mm$< z <$ 150 mm) during the calculation of the ACF in Fig 3F. To obtain the characteristic reorientation timescales (τ) of wild–type ($\tau = 0.38 \pm 0.02$ s) and mutant fish ($\tau = 0.80 \pm 0.05$ s), ACFs were fitted with an exponential function, $C(t) = A \exp(-t/\tau)$ where $A(\leq 1)$ is a constant. Our results thus show that mutant fish take longer to change their direction of movement than the wild–type fish. The difference in the reorientation timescale was robust across successive measurements, as we repeated the experiment using zebrafish bred independently and obtained same results (see section V of S1 Text for details on the experiments).

A group of mutant fish exhibit more ordered motion

How does the change in the individual swimming pattern affect the behaviour of a group? To answer this question, we recorded the collective motion of 25 zebrafish in the same 3d tracking apparatus as that shown in Fig 3A. We studied the fish at a variety of ages from 40 dpf (days post fertilisation) to 120 dpf, to capture the effects of fish development [66] and repeated exposure to the experimental environment [67]. This way, we can probe the swimming behaviour at different developmental times of zebrafish.

Even if we completely discard these developmental effects, by concatenating all the results together, we still find a significant difference between the mutant fish group and the wild–type group. The analysis of such a merged dataset is shown in Fig 3D, 3G and 3H. These differences are similar to those observed in the one–fish experiments. Again the wild–type fish tended to be distributed at the bottom of the tank, exhibiting a bimodal speed distribution. When calculating the average orientational relaxation time (τ) of individual fish in the group, the mutant fish group also presents a higher value ($\tau = 0.33 \pm 0.04s$), compared to the wild–type group ($\tau = 0.20 \pm 0.01s$). The difference between a group of the wild–type fish and the mutant fish is more significant if we compare the two groups in a specific age, as shown in Fig S6 in S1 Text.

Strikingly, groups of mutant fish exhibit more ordered motion, as shown in Fig 3I. The degree of order of the motion is characterised by the *polarization* (Φ), a dynamical order parameter with the following definition,

$$\Phi = \frac{1}{N}\left|\sum_i \frac{\mathbf{v}_i}{|\mathbf{v}_i|}\right|, \tag{1}$$

where N is the number of fish in the group, and $\mathbf{v}_i$ represents the velocity of the ith fish in the group. The value of Φ approaches unity if all the fish swim in the same direction and zero in the case that the swim directions are random. The distribution of Φ for mutant fish is significantly shifted towards larger values, suggesting that the collective behaviour of mutant fish is more ordered. This difference is visually obvious as shown in the S1 Video. To exclude the possibility that the behavioural difference between the wild–type group and the mutant group was caused by the bowl–shaped container, we performed more analysis while conditioning the fish to be inside a narrow and fixed spatial range. The results are in section IV in S1 Text. Regardless of the swimming location, there is a consistent behavioural difference between the wild–type and the mutant fish.

The collective behaviour of mutants can be modelled by a modified Vicsek model

The increase in ordering in the case of the *col11a2 -/-* zebrafish, compared to the wild–type may be explored in the context of the Vicsek model [15], which exhibits an order to disorder transition with the increase of orientational randomness or the decrease of number density. The Vicsek model is a minimal model where the simulated agents only interact with each other via local orientational alignment, and this model can be modified to match the fish behaviour, simply by adding an inertial term such that the velocity $\mathbf{v}_i$ of each agent (fish) is updated as, [27]

$$\mathbf{v}_i(t+1) = v_0\Theta\left[(1-\alpha)\ \underbrace{v_0\mathcal{R}_\eta\left[\Theta\left(\sum_{j\in S_i}\mathbf{v}_j(t)\right)\right]}_{\text{Vicsek Model}} + \alpha\mathbf{v}_i(t)\right], \tag{2}$$

where v_0 represents the constant self–propelling speed for all agents. Θ normalises the velocity vector, such that the constant velocity condition is maintained. Noise in the direction of motion is implemented with $\mathcal{R}_\eta$ such that the velocity vector falls on a spherical cap of amplitude $4\pi\eta$ with η controlling the strength of the noise [27]. The parameter α takes the value between 0 and 1, and effectively adjusts the inertia of the agents, so that those with larger α values change their orientations more slowly. Essentially, the velocities for all agents in time point $t + 1$, $\mathbf{v}(t + 1)$, are mixtures of the Vicsek updating results, as well as their respective velocities in time point t, $\mathbf{v}(t)$. Such "memory" in terms of velocities gives the agents effective inertia in their orientations, which prevents the agents from performing unrealistically fast reorientations. The value of α in Eq 2 changes the relative proportion of the two, and we set its value to be 0.63, consistent with previous work [40]. In our discussion on the effect of the α value of the model is available in section III of S1 Text, we conclude that the $\alpha = 0.63$ fitted to our data provides convincing evidence for some effective inertia in the zebrafish system.

The model generates 3d trajectories that can be compared to the experimental data. Such comparison can be made easy if we measure dimensionless quantities from both simulations and experiments, as we can therefore ignore biological details such as the body length of the fish. Here we focus on the *reduced persistence length*, defined as the ratio between the persistence length l_p, and the average nearest neighbor distance l_{nn}. The persistence length l_p is the product of the orientation relaxation time τ and the speed of the fish/agents, averaged between all individuals. The value of l_{nn} is calculated by averaging the distances of all fish/agents to their closest neighbors. Both l_p and l_{nn} have units of length so that their ratio is dimensionless. With these measures in hand, we now proceed to investigate whether the *col11a2 -/-* zebrafish may similarly be described with the same model.

In Fig 4A, we plot the values of persistence length (l_p) and nearest neighbour distance (l_{nn}) for both the mutant (squares) and wild–type (circles) fish. We see that the mutant fish have both larger l_{nn} and l_p values. The larger l_{nn} values of the mutant fish reflect their distribution in the upper location of the tank, of naturally larger volume given the geometry of the tank. The larger l_p of the mutant fish is presumably related to their slow re-orientation, as the persistence length l_p is defined as the product of the speed and the orientational relaxation time. With the aging of the zebrafish, the average l_{nn} decreased for both the wild–type group and the mutant group, indicating that the fish exhibited more cohesive behaviour as they grew from 43 dpf to over 100 dpf. This increasing local density amongst zebrafish was also observed by Buske and Gerlai, and could be related to ecological factors such as avoiding predators, mating, or food

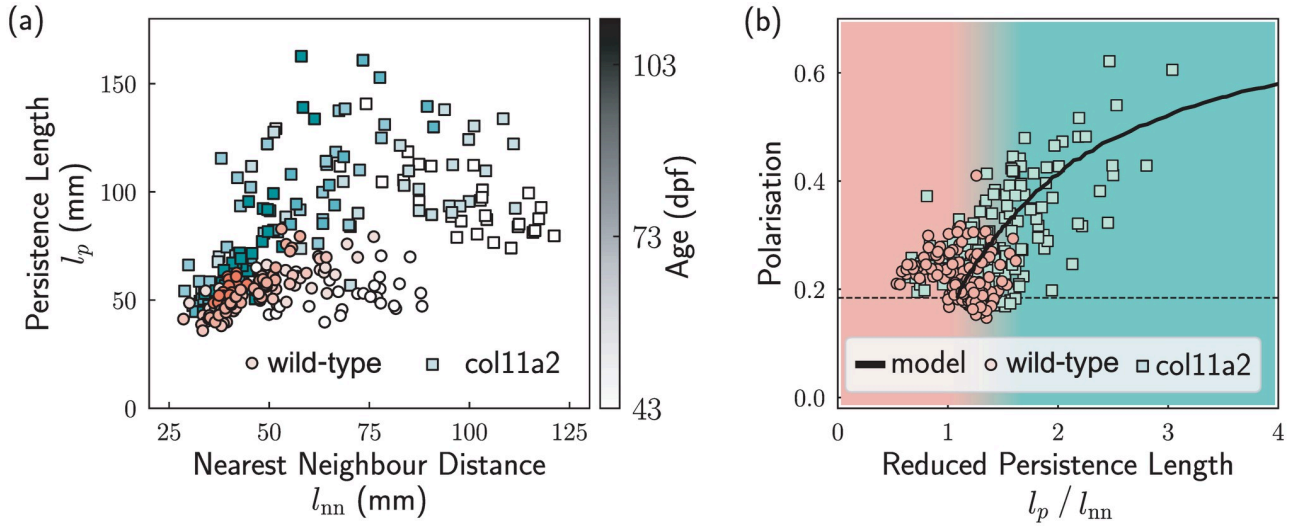

Fig 4. Important lengthscales of 25 wild–type fish (◯) and mutant fish (□). (a) The nearest neighbour distance and the persistence length for the fish. Each scatter represents the average value in 2 minutes, whose grayscale values represent the age of the fish. (b) The relationship between the group polarisation and the reduced persistence length values. The data points represent the experiments and the line represents the simulation result where the fish obey the updating rule in Eq 2. The shading represents the regimes of the reduced persistence length which are dominated by the wild–type (red) and mutant (green). The dashed line represents the expected polarization of 25 randomly orientated vectors.

https://doi.org/10.1371/journal.pcbi.1012034.g004

discovery [68]. For juvenile fish (ages from 43 to 103 dpf), whether wild–type or mutant, a correlation between l_p/l_{nn} and Φ was also observed, as shown in Fig 4B. The mutant fish have a larger reduced persistence length compared with wild–type fish, which is correlated with higher polarisation.

The simulation results of the model provide a good fit for the experimental results, as shown in Fig 4B. To obtain different persistence length values, we changed the orientational noise of each individual agent. The match of the experimental data to the model suggests that the fish were effectively aligned with each other. Such alignment interaction enables the fish group to access an ordered state with high polarisation. The lack of *col11a2* caused defects in their spines, changed their swimming postures, and resulted in slower re–orientation of individuals, hence increasing the persistent length l_p of the group. The increase of l_p for a group of mutant fish yields more ordered movement for the presence of the aligning interaction. Nevertheless, at the level of our analysis, these changes in behaviour can be described with the same model we used previously. In short, the same modified Vicsek model (with the same value for the inertia parameter α) fits both wild–type and *col11a2 -/-* zebrafish. In the context of this model, the mutants sample, on average, a different region of state space, although the distributions between the two types of fish do overlap.

To the best of our knowledge, this is the first report of the explicit linkage between the macroscopic phenomena (group polarisation) of the animal collective behaviour, and the microscopic detail of the individual animal (spinal defects and changed swimming posture) which we control with genetic modification. We explained such linkage with a modified Vicsek model, that the longer persistence length of the mutant fish can be mapped to a lower re–orientation noise in the model. It is notable that Vicsek model is a famously minimalistic model that is unable to explain all the observed fish behaviour. More sophisticated models [49, 69–71] should be used to fit our experimental data to yield better explanations and more insights. However, an exhaustive comparison for all models are beyond the scope of this study.

Discussion

Knocking out the *col11a2* gene changes the zebrafish system at the level of the individual fish, in several ways. The gene regulates the expression of the collagen, and its absence leads to defects in their vertebrae and intervertebral discs. Consequently, the mutant fish exhibit less bending during swimming compared to the wild–type fish, especially when the speed is slow. The compromised spinal development and bending ability are likely to prevent the mutant fish from making frequent directional changes when swimming, leading to a longer orientational relaxation time. Effectively, the *col11a2* -/- zebrafish exhibited less "orientational noise", if they were modelled as self–propelling agents with aligning interactions. On the group level, the reduced noise value is captured by the increased persistence length. A group of mutant fish is then expected to swim in a more ordered manner, where all the fish are likely to swim towards the same direction. This expectation is consistent with our observations for groups ($N = 25$) of wild–type fish and *col11a2* -/- fish. In other words, we can use the genetic modification to tune the fish behaviour in a way which can be interpreted with a simple physical model.

The behaviour of animals in a group with moderate size, is affected by both the microscopic details of individuals and the interaction between individuals. In our study, the collective motion of 25 fish is affected by the microscopic, single–fish property, as shown in Fig 3. Nevertheless, the fish–fish interaction also triggered a significant difference in the group polarization (Figs 3I and 4). For biological purposes, the microscopic single–fish features are useful measurements of the phenotypic response to the genetic modification. In this study, we followed this "biological path" extensively by looking into the single–fish behaviour as well as the bone structures of the fish. On the other hand, we expect the knockout of the *col11a2* gene to trigger a larger response in a larger group, since the discontinuous nature of the dynamical order–disorder transition [17, 28] will be blurred out in a small group, as a consequence of the finite-size effect [72]. However, performing such an experiment with a large group of mutant fish is challenging, as mutants display a relatively high mortality rate. In addition, tracking larger groups requires better camera systems (see [73] for example), more optimised algorithms (see [74, 75] for examples), and a very large space to avoid the interruption from the boundary. These requirements are beyond our current experimental capability. Nevertheless, we would expect a large group of wild–type fish to stay in the order-disorder transition region to enjoy the maximum susceptibility [40, 76, 77], while a large group of mutant fish are expected to reside on the ordered region.

Conclusion

Our work describes a quantitative study on the behavioural difference between wild–type zebrafish and the *col11a2* -/- zebrafish whose *col11a2* gene is knocked out (suppressed). The genetic modification caused defects in the vertebral column of mutants, leading to less body–bending in swimming, hence a slower reorientation process. This behavioural difference of a single fish affected the group behaviour of twenty five, where the mutant fish group exhibited more ordered collective motion that correlates with their more persistent swimming style. In other words, we have tuned the behaviour of a biological system in a manner reminiscent of synthetic colloids or *de novo* proteins. This is interpreted as the mutant fish system adopting a different state space with respect to the wild–type in the context of a minimalistic physical model. In particular the difference between mutant and wild–type fish can be summarised by different orientational noise level in a modified Vicsek model. Taken together we have shown that by modelling the swimming behaviour of zebrafish and treating them as active matter, we can reveal physiologically relevant behaviours that are underpinned by changes to the skeleton,

demonstrating the utility of this approach as a tool to follow genetic mutants and relate behaviours to genetic traits and to phsyiological changes within the body.

Supporting information

S1 Text. Extra analysis on the difference between mutant and wildtype zebrafish, and extra details on the methodology. The differences of the otoliths between the fish and the wildtype zebrafish, the analysis on the swimming location of the fish, the effect of parameter α in the simulation, more details on the shape–bending analysis of the zebrafish, and more details on the experimental procedure.
(PDF)

S1 Video. The movements of 25 mutant fish and wildtype fish. The wildtype fish exhibited random movelment with a low polarization value, while the mutant fish perform an ordered movement with a higher polarization value.
(MOV)

Acknowledgments

JL Ross Anderson is gratefully thanked for discussions and YY thanks Min Wang for the help with editing the supplementary video.

Author Contributions

Conceptualization: Yushi Yang, Abdelwahab Kawafi, Erika Kague, Chrissy L. Hammond, C. Patrick Royall.

Data curation: Yushi Yang, Abdelwahab Kawafi, Qiao Tong, C. Patrick Royall.

Formal analysis: Yushi Yang, Abdelwahab Kawafi, Qiao Tong, Chrissy L. Hammond.

Funding acquisition: Erika Kague, Chrissy L. Hammond, C. Patrick Royall.

Investigation: Yushi Yang, Erika Kague, Chrissy L. Hammond, C. Patrick Royall.

Methodology: Yushi Yang, Abdelwahab Kawafi, Erika Kague, Chrissy L. Hammond, C. Patrick Royall.

Project administration: Erika Kague, Chrissy L. Hammond, C. Patrick Royall.

Resources: Erika Kague, Chrissy L. Hammond, C. Patrick Royall.

Software: Yushi Yang, Abdelwahab Kawafi, Erika Kague, C. Patrick Royall.

Supervision: Erika Kague, Chrissy L. Hammond, C. Patrick Royall.

Validation: Yushi Yang, Abdelwahab Kawafi, Chrissy L. Hammond, C. Patrick Royall.

Visualization: Yushi Yang, Abdelwahab Kawafi.

Writing – original draft: Yushi Yang, Abdelwahab Kawafi, Erika Kague, Chrissy L. Hammond, C. Patrick Royall.

Writing – review & editing: Yushi Yang, Abdelwahab Kawafi, Erika Kague, Chrissy L. Hammond, C. Patrick Royall.

References

1. Parrish JK, Edelstein-Keshet L. Complexity, Pattern, and Evolutionary Trade-Offs in Animal Aggregation. Science. 1999; 284(5411):99–101. https://doi.org/10.1126/science.284.5411.99 PMID: 10102827

2. Cavagna A, Cimarelli A, Giardina I, Parisi G, Santagati R, Stefanini F, et al. Scale-Free Correlations in Starling Flocks. Proceedings of the National Academy of Sciences of the United States of America. 2010; 107(26):11865–11870. https://doi.org/10.1073/pnas.1005766107 PMID: 20547832

3. Silverberg JL, Bierbaum M, Sethna JP, Cohen I. Collective Motion of Humans in Mosh and Circle Pits at Heavy Metal Concerts. Physical Review Letters. 2013; 110(22):617–5. https://doi.org/10.1103/PhysRevLett.110.228701 PMID: 23767754

4. Miller N, Gerlai R. From Schooling to Shoaling: Patterns of Collective Motion in Zebrafish (Danio Rerio). PLoS ONE. 2012; 7(11):e48865. https://doi.org/10.1371/journal.pone.0048865 PMID: 23166599

5. Tunstrøm K, Katz Y, Ioannou CC, Huepe C, Lutz MJ, Couzin ID. Collective States, Multistability and Transitional Behavior in Schooling Fish. PLoS Computational Biology. 2013; 9(2):e1002915. https://doi.org/10.1371/journal.pcbi.1002915 PMID: 23468605

6. Sinhuber M, van der Vaart K, Ouellette NT. Response of insect swarms to dynamic illumination perturbations. Journal of The Royal Society Interface. 2019; 16(150):20180739. https://doi.org/10.1098/rsif.2018.0739 PMID: 30958145

7. Deneubourg JL, Goss S. Collective Patterns and Decision-Making. Ethology Ecology & Evolution. 1989; 1(4):295–311. https://doi.org/10.1080/08927014.1989.9525500

8. Vicsek T, Zafeiris A. Collective Motion. Physics Reports. 2012; 517(3-4):71–140. https://doi.org/10.1016/j.physrep.2012.03.004

9. Cavagna A, Giardina I. Bird Flocks as Condensed Matter. Annual Review of Condensed Matter Physics. 2014; 5(1):183–207. https://doi.org/10.1146/annurev-conmatphys-031113-133834

10. Magurran AE. The Adaptive Significance of Schooling as an Anti-Predator Defence in Fish. In: Annales Zoologici Fennici. JSTOR; 1990. p. 51–66.

11. Hemelrijk C, Reid D, Hildenbrandt H, Padding J. The increased efficiency of fish swimming in a school. Fish and Fisheries. 2015; 16(3):511–521. https://doi.org/10.1111/faf.12072

12. Ramdya P, Lichocki P, Cruchet S, Frisch L, Tse W, Floreano D, et al. Mechanosensory Interactions Drive Collective Behaviour in Drosophila. Nature. 2015; 519(7542):233–236. https://doi.org/10.1038/nature14024 PMID: 25533959

13. Demartsev V, Strandburg-Peshkin A, Ruffner M, Manser M. Vocal Turn-Taking in Meerkat Group Calling Sessions. Current Biology. 2018; 28(22):3661–3666.e3. https://doi.org/10.1016/j.cub.2018.09.065 PMID: 30416063

14. Ling H, Mclvor GE, Westley J, Vaart K, Vaughan RT, Thornton A, et al. Behavioural Plasticity and the Transition to Order in Jackdaw Flocks. Nature Communications. 2019; p. 1–7. https://doi.org/10.1038/s41467-019-13281-4 PMID: 31729384

15. Vicsek T, Czirok A, Benjacob E, Cohen I, Shochet O. Novel Type of Phase-Transition in a System of Self-Driven Particles. Phys Rev Lett. 1995; 75(6):1226–1229. https://doi.org/10.1103/PhysRevLett.75.1226 PMID: 10060237

16. Bechinger C, Leonardo RD, Löwen H, Reichhardt C, Volpe G, Volpe G. Active Particles in Complex and Crowded Environments. Reviews of Modern Physics. 2016; 88(4):045006. https://doi.org/10.1103/RevModPhys.88.045006

17. Solon AP, Chaté H, Tailleur J. From Phase to Microphase Separation in Flocking Models: The Essential Role of Nonequilibrium Fluctuations. Physical Review Letters. 2015; 114(6):068101. https://doi.org/10.1103/PhysRevLett.114.068101 PMID: 25723246

18. Ramaswamy S. Active Matter. Journal of Statistical Mechanics: Theory and Experiment. 2017; 2017(5):054002. https://doi.org/10.1088/1742-5468/aa6bc5

19. Rahmani P, Peruani F, Romanczuk P. Topological Flocking Models in Spatially Heterogeneous Environments. Communications Physics. 2021; 4(1):206. https://doi.org/10.1038/s42005-021-00708-y

20. Couzin ID, Krause J, James R, Ruxton GD, Franks NR. Collective memory and spatial sorting in animal groups. Journal of Theoretical Biology. 2002; 218(1):1–11. https://doi.org/10.1006/jtbi.2002.3065 PMID: 12297066

21. Cavagna A, Castello LD, Giardina I, Grigera T, Jelic A, Melillo S, et al. Flocking and Turning: A New Model for Self-Organized Collective Motion. Journal of Statistical Physics. 2015; 158(3):601–627. https://doi.org/10.1007/s10955-014-1119-3

22. Bastien R, Romanczuk P. A Model of Collective Behavior Based Purely on Vision. Science Advances. 2020; 6(6):eaay0792. https://doi.org/10.1126/sciadv.aay0792 PMID: 32076645

23. Kaiser A, Snezhko A, Aranson IS. Flocking Ferromagnetic Colloids. Science Advances. 2017; 3(2):e1601469. https://doi.org/10.1126/sciadv.1601469 PMID: 28246633

24. Geyer D, Morin A, Bartolo D. Sounds and Hydrodynamics of Polar Active Fluids. Nature Materials. 2018; 17(9):789–793. https://doi.org/10.1038/s41563-018-0123-4 PMID: 29967463

25. Jia Y, Wang L. Leader Follower Flocking of Multiple Robotic Fish. IEEE/ASME Transactions on Mechatronics. 2015; 20(3):1372–1383. https://doi.org/10.1109/TMECH.2014.2337375

26. Ordaz-Rivas E, Rodriguez-Liñan A, Torres-Treviño L. Flock of Robots with Self-Cooperation for Prey-Predator Task. Journal of Intelligent & Robotic Systems. 2021; 101(2):39. https://doi.org/10.1007/s10846-020-01283-0

27. Ginelli F. The Physics of the Vicsek model. Eur Phys J Special Topics. 2016; 225:2099–2117. https://doi.org/10.1140/epjst/e2016-60066-8

28. Martin D, Chaté H, Nardini C, Solon A, Tailleur J, Van Wijland F. Fluctuation-Induced Phase Separation in Metric and Topological Models of Collective Motion. Physical Review Letters. 2021; 126(14):148001. https://doi.org/10.1103/PhysRevLett.126.148001 PMID: 33891435

29. Romenskyy M, Herbert-Read JE, Ioannou CC, Szorkovszky A, Ward AJW, Sumpter DJT. Quantifying the structure and dynamics of fish shoals under predation threat in three dimensions. Behavioral Ecology. 2020; 31:311–321. https://doi.org/10.1093/beheco/arz197

30. Patel ML, Ouellette NT. Formation and dissolution of midge swarms. Physical Review E. 2022; 105(3):034601. https://doi.org/10.1103/PhysRevE.105.034601 PMID: 35428071

31. Bricard A, Caussin JB, Desreumaux N, Dauchot O, Bartolo D. Emergence of macroscopic directed motion in populations of motile colloids. Nature. 2013; 503(7474):95–98. https://doi.org/10.1038/nature12673 PMID: 24201282

32. Yan J, Han M, Zhang J, Xu C, Luijten E, Granick S. Reconfiguring active particles by electrostatic imbalance. Nature Materials. 2016; 15(10):1095–1099. https://doi.org/10.1038/nmat4696 PMID: 27400388

33. Buttinoni I, Bialké J, Kümmel F, Löwen H, Bechinger C, Speck T. Dynamical clustering and phase separation in suspensions of self-propelled colloidal particles. Physical Review Letters. 2013; 110(23):238301. https://doi.org/10.1103/PhysRevLett.110.238301 PMID: 25167534

34. Klongvessa N, Ginot F, Ybert C, Cottin-Bizonne C, Leocmach M. Active Glass: Ergodicity Breaking Dramatically Affects Response to Self-Propulsion. Physical Review Letters. 2019; 123(24):248004. https://doi.org/10.1103/PhysRevLett.123.248004 PMID: 31922864

35. Lavergne FA, Wendehenne H, Bäuerle T, Bechinger C. Group formation and cohesion of active particles with visual perception–dependent motility. Science. 2019; 364(6435):70–74. https://doi.org/10.1126/science.aau5347 PMID: 30948548

36. Morfill GE, Ivlev A. Complex plasmas: An interdisciplinary research field. Rev Mod Phys. 2009; 81:1353–1404. https://doi.org/10.1103/RevModPhys.81.1353

37. Huang PS, Boyken SE, Baker D. The coming of age of de novo protein design. Nature. 2016; 537:320–327. https://doi.org/10.1038/nature19946 PMID: 27629638

38. Favre-Bulle IA, Stilgoe AB, Rubinsztein-Dunlop H, Scott EK. Optical Trapping of Otoliths Drives Vestibular Behaviours in Larval Zebrafish. Nature Communications. 2017; 8(1):630. https://doi.org/10.1038/s41467-017-00713-2 PMID: 28931814

39. Li L, Nagy M, Graving JM, Bak-Coleman J, Xie G, Couzin ID. Vortex Phase Matching as a Strategy for Schooling in Robots and in Fish. Nature Communications. 2020; 11(1):5408. https://doi.org/10.1038/s41467-020-19086-0 PMID: 33106484

40. Yang Y, Turci F, Kague E, Hammond CL, Russo J, Royall CP. Dominating Lengthscales of Zebrafish Collective Behaviour. PLOS Computational Biology. 2022; 18(1):1–14. https://doi.org/10.1371/journal.pcbi.1009394 PMID: 35025883

41. Gerlai R. Fish in Behavior Research: Unique Tools with a Great Promise! Journal of Neuroscience Methods. 2014; 234:54–58. https://doi.org/10.1016/j.jneumeth.2014.04.015 PMID: 24768578

42. Kim OH, Cho HJ, Han E, Hong TI, Ariyasiri K, Choi JH, et al. Zebrafish Knockout of Down Syndrome Gene, DYRK1A, Shows Social Impairments Relevant to Autism. Molecular Autism. 2017; 8(1):50. https://doi.org/10.1186/s13229-017-0168-2 PMID: 29021890

43. Salazar-Silva R, Dantas VLG, Alves LU, Batissoco AC, Oiticica J, Lawrence EA, et al. NCOA3 identified as a new candidate to explain autosomal dominant progressive hearing loss. Human Molecular Genetics. 2020; 29(22):3691–3705. https://doi.org/10.1093/hmg/ddaa240

44. Kague E, Turci F, Newman E, Yang Y, Brown KR, Aglan MS, et al. 3D Assessment of Intervertebral Disc Degeneration in Zebrafish Identifies Changes in Bone Density That Prime Disc Disease. Bone Research. 2021; p. 1–17. https://doi.org/10.1038/s41413-021-00156-y PMID: 34465741

45. Tang W, Davidson JD, Zhang G, Conen KE, Fang J, Serluca F, et al. Genetic Control of Collective Behavior in Zebrafish. iScience. 2020; 23(3):100942. https://doi.org/10.1016/j.isci.2020.100942 PMID: 32179471

46. Harpaz R, Aspiras AC, Chambule S, Tseng S, Bind MA, Engert F, et al. Collective Behavior Emerges from Genetically Controlled Simple Behavioral Motifs in Zebrafish. Science Advances. 2021; 7(41): eabi7460. https://doi.org/10.1126/sciadv.abi7460 PMID: 34613782

47. Degond P, Motsch S. Large Scale Dynamics of the Persistent Turning Walker Model of Fish Behavior. Journal of Statistical Physics. 2008; 131(6):989–1021. https://doi.org/10.1007/s10955-008-9529-8

48. Zienkiewicz A, Barton DAW, Porfiri M, Bernardo Md. Data-driven stochastic modelling of zebrafish locomotion. Journal of Mathematical Biology. 2015; 71(5):1081–1105. https://doi.org/10.1007/s00285-014-0843-2 PMID: 25358499

49. Klamser PP, Gómez-Nava L, Landgraf T, Jolles JW, Bierbach D, Romanczuk P. Impact of Variable Speed on Collective Movement of Animal Groups. Frontiers in Physics. 2021; 9. https://doi.org/10.3389/fphy.2021.715996

50. Gautrais J, Ginelli F, Fournier R, Blanco S, Soria M, Chaté H, et al. Deciphering interactions in moving animal groups. PLoS Computational Biology. 2012; 8(9):e1002678. https://doi.org/10.1371/journal.pcbi.1002678 PMID: 23028277

51. Filella A, Nadal F, Sire C, Kanso E, Eloy C. Model of collective fish behavior with hydrodynamic interactions. Physical Review Letters. 2018; 120(19):198101. https://doi.org/10.1103/PhysRevLett.120.198101 PMID: 29799263

52. Lawrence EA, Kague E, Aggleton JA, Harniman RL, Roddy KA, Hammond CL. The mechanical impact of col11a2 loss on joints; col11a2 mutant zebrafish show changes to joint development and function, which leads to early-onset osteoarthritis. Philos Trans R Soc Lond B Biol Sci. 2018; 373 (1759). https://doi.org/10.1098/rstb.2017.0335 PMID: 30249781

53. Westerfield M. The zebrafish book: A guide for the laboratory use of zebrafish (danio rerio). University of Oregon Press; 2000.

54. Walker DM, Kimmel C. A two-color acid-free cartilage and bone stain for zebrafish larvae. Biotechnic & Histochemistry. 2007; 82(1):23–28. https://doi.org/10.1080/10520290701333558 PMID: 17510811

55. Kague E, Witten PE, Soenens M, Campos C, Lubiana T, Fisher S, et al. Zebrafish sp7 mutants show tooth cycling independent of attachment, eruption and poor differentiation of teeth. Developmental Biology. 2018; 435(2):176–184. https://doi.org/10.1016/j.ydbio.2018.01.021 PMID: 29409769

56. Chen X, Nadiarynkh O, Plotnikov S, Campagnola PJ. Second harmonic generation microscopy for quantitative analysis of collagen fibrillar structure. Nature Protocols. 2012; 7(4):654–669. https://doi.org/10.1038/nprot.2012.009 PMID: 22402635

57. Hartley R, Zisserman A. Multiple View Geometry in Computer Vision. 2nd ed. USA: Cambridge University Press; 2003.

58. Ouellette NT, Xu H, Bodenschatz E. A Quantitative Study of Three-Dimensional Lagrangian Particle Tracking Algorithms. Experiments in Fluids. 2005; 40(2):301–313. https://doi.org/10.1007/s00348-005-0068-7

59. Xu H. Tracking Lagrangian Trajectories in Position–Velocity Space. Measurement Science and Technology. 2008; 19(7):075105. https://doi.org/10.1088/0957-0233/19/7/075105

60. Cavagna A, Giardina I, Orlandi A, Parisi G, Procaccini A, Viale M, et al. The STARFLAG handbook on collective animal behaviour: 1. Empirical methods. Animal Behaviour. 2008; 76(1):217–236. https://doi.org/10.1016/j.anbehav.2008.02.003

61. Hayes AJ, Benjamin M, Ralphs JR. Extracellular Matrix in Development of the Intervertebral Disc. Matrix Biology. 2001; 20(2):107–121. https://doi.org/10.1016/S0945-053X(01)00125-1 PMID: 11334712

62. Williams RM, Zipfel WR, Webb WW. Interpreting Second-Harmonic Generation Images of Collagen I Fibrils. Biophysical Journal. 2005; 88(2):1377–1386. https://doi.org/10.1529/biophysj.104.047308 PMID: 15533922

63. Li G, Kolomenskiy D, Liu H, Godoy-Diana R, Thiria B. Intermittent versus continuous swimming: An optimization tale. Phys Rev Fluids. 2023; 8:013101. https://doi.org/10.1103/PhysRevFluids.8.013101

64. Butail S, Paley DA. Three-dimensional reconstruction of the fast-start swimming kinematics of densely schooling fish. Journal of The Royal Society Interface. 2011; 9(66):77–88. https://doi.org/10.1098/rsif.2011.0113 PMID: 21642367

65. Allen MP, Tildesley DJ. Computer simulation of liquids. OUP Oxford; 2017.

66. Hinz RC, Polavieja GGd. Ontogeny of collective behavior reveals a simple attraction rule. Proceedings of the National Academy of Sciences. 2017; 114(9). https://doi.org/10.1073/pnas.1616926114 PMID: 28193864

67. MacGregor HEA, Ioannou CC. Emergence of variation between groups through time in fish shoal collective motion. bioRxiv. 2021. https://doi.org/10.1101/2021.02.23.432454

68. Buske C, Gerlai R. Shoaling develops with age in Zebrafish (Danio rerio). Progress in Neuro-Psychopharmacology and Biological Psychiatry. 2011; 35(6):1409–1415. https://doi.org/10.1016/j.pnpbp.2010.09.003 PMID: 20837077

69. Calovi DS, Lopez U, Ngo S, Sire C, Chaté H, Theraulaz G. Swarming, schooling, milling: phase diagram of a data-driven fish school model. New Journal of Physics. 2014; 16(1):015026. https://doi.org/10.1088/1367-2630/16/1/015026

70. Ito S, Uchida N. Selective decision making and collective behavior of fish by the motion of visual attention; 2024. Available from: http://arxiv.org/abs/2402.09073.

71. Puy A, Gimeno E, Torrents J, Bartashevich P, Miguel MC, Pastor-Satorras R, et al. Selective social interactions and speed-induced leadership in schooling fish. Proceedings of the National Academy of Sciences. 2024; 121(18):e2309733121. https://doi.org/10.1073/pnas.2309733121 PMID: 38662546

72. Newman MEJ, Barkema GT. Monte Carlo Methods in Statistical Physics. Clarendon Press; 1999.

73. Cavagna A, Feng X, Melillo S, Parisi L, Postiglione L, Villegas P. CoMo: A Novel Comoving 3D Camera System. IEEE Transactions on Instrumentation and Measurement. 2021; 70:1–16. https://doi.org/10.1109/TIM.2021.3074388

74. Romero-Ferrero F, Bergomi MG, Hinz R, Heras FJH, de Polavieja GG. Idtracker.Ai: Tracking All Individuals in Large Collectives of Unmarked Animals. arXiv. 2018;cs.CV:arXiv:1803.04351.

75. Walter T, Couzin ID. TRex, a Fast Multi-Animal Tracking System with Markerless Identification, and 2D Estimation of Posture and Visual Fields. bioRxiv. 2021; p. 2020.10.14.338996. https://doi.org/10.1101/2020.10.14.338996

76. Mora T, Bialek W. Are Biological Systems Poised at Criticality? Journal of Statistical Physics. 2011; 144(2):268–302. https://doi.org/10.1007/s10955-011-0229-4

77. Muñoz MA. Colloquium: Criticality and Dynamical Scaling in Living Systems. Reviews of Modern Physics. 2018; 90(3):031001. https://doi.org/10.1103/RevModPhys.90.031001